

Two-dimensional gratings for low polarization dependent wavelength demultiplexing

John Hoose¹ and Evgeny Popov^{2,*}

¹14 Dewey Avenue, Fairport, New York 14450, USA

²Institut Fresnel, Unité mixte de recherche de CNRS 6133, Aix-Marseille Université, avenue Escadrille Normandie-Niemen, 13397 Marseille, Cedex 20, France

*Corresponding author: e.popov@fresnel.fr

Received 22 May 2008; revised 8 July 2008; accepted 11 July 2008;
posted 15 July 2008 (Doc. ID 96571); published 28 August 2008

Two-dimensional (crossed) diffraction gratings with sinusoidal or truncated pyramidal (trapezoidal) profiles are proposed to have diffraction efficiency almost independent of the incident polarization inside the optical communication spectral window 1.5–1.6 μm . The gratings are characterized by different periods in the two orthogonal directions, chosen to support only one dispersive diffraction order in addition to the zeroth (specular) one. © 2008 Optical Society of America

OCIS codes: 060.4230, 050.1950, 050.2770.

1. Introduction

The search for high-efficiency low-polarization dependent diffraction gratings is motivated by the rapid development of high density optical communication wavelength multiplexing. With the extensive research in integrated optics from the 70s to the mid-90s, many compact integrated optical devices were proposed but very few obtained commercial success. The interested reader can find many interesting designs summarized in Refs. [1,2]. Recently, the interest in integrated systems has been revived again with the development of nanotechnologies [3,4]. However, waveguide gratings yet fail to show efficiency performance comparable to the classical relief gratings. Large-period echelles [2] can have efficiency in unpolarized light exceeding 90% but are limited by the change in the blazing diffraction order with the wavelength. Short-period reflection gratings can have a plateaulike spectral dependence in TM polarization (magnetic field parallel to the grooves), but the TE peak comes at shorter wavelengths. The reduction of the polarization dependence can be done by using deeper gratings, either in reflection [5] or transmission [6] but is limited when higher-

incident angles are required to increase the dispersion, as shown in Section 2. Using photonic crystals as dispersive optical elements has been proposed only recently [7]. When working inside the zone forbidden both in TE and TM polarization, one can obtain high values of efficiency within a spectral domain almost covering the entire forbidden gap, which seems attractive for telecom applications [7,8]. Negative refraction properties have also been studied for high-efficiency demultiplexing [9,10]. The main problem with photonic crystals is their practical realization and low-cost implementation in the visible and near infrared domain. Another possibility consists in combining properties of known commercial gratings [11,12], or using gratings etched in silicon having a naturally sharp apex angle [13]. Although the latter example provides all the properties required for dense wavelength demultiplexing, its configuration imposes use of a bulk silicon prism, which can be of some practical inconvenience.

The aim of this paper is to analyze the diffraction properties of specific crossed gratings. The existence of a double periodicity in two different directions gives several more degrees of freedom to optimize the efficiency behavior. We consider two different grating profiles, double-sinusoidal grooves, and truncated pyramidal bumps. In Section 2, we briefly analyze

the properties of deep, one-dimensional (1D), sinusoidal gratings to show their limitations at higher angles of incidence. Section 3 introduces the geometry under consideration, together with the optimal profiles for double-sinusoidal profiles at two different incident angles, 60° and 70°. Section 4 presents the results for a grating consisting of truncated pyramidal bumps.

2. Deep One-Dimensional Grating Efficiency

As already discussed, it is possible to simultaneously obtain high efficiency in both TE and TM polarization by using classical (one-dimensional) reflection gratings, provided the grooves are sufficiently deep. Figures 1(a)–1(c) represent the efficiency of a sinusoidal-profile, 1D, gold grating.

The first example concerns a configuration which works around the Littrow mount at wavelength 1.55 μm at a 40° angle of incidence. The groove depth dependence in Fig. 1(a) shows the possibility to obtain equal TE and TM efficiency with relatively deep grooves (groove depth-to-period ratio $h/d = 1.128$). Although the spectral dependence behaves in an opposite manner in both polarization, an overall acceptable result can be achieved within the working spectral interval, Fig. 1(b). However, when higher angular dispersion is required (shorter period and larger incident

angle), it is not possible to achieve efficiency higher enough in TE polarization, as observed in Fig. 1(c).

The numerical results presented here are obtained using a method based on a curvilinear transformation of the coordinate system, a method known under the name ‘C-method’ [14–16]. Its performance is independent of the incident polarization and grating material conductivity, and the formulation proposed by Li [16] overcomes its implicit difficulty to deal with profiles having edges, an amelioration decisive for being able to obtain the results given in Section 4 for pyramidal structures.

3. Diffraction Efficiency of Two-Dimensional Sinusoidal Grating

To overcome the difficulties for 1D gratings, discussed in Section 2, we propose to consider, at first, a 2D grating with a profile represented as a sum of two sinusoids:

$$f(x, z) = \frac{h_x}{2} \sin(K_x x) + \frac{h_z}{2} \sin(K_z z), \quad (1)$$

with groove depth values h_x and h_z , and groove numbers given by the corresponding periods, $K_x = 2\pi/d_x$, $K_z = 2\pi/d_z$. The grating lies in the xOz plane, and the two axes along the 2D periodicity are orthogonal

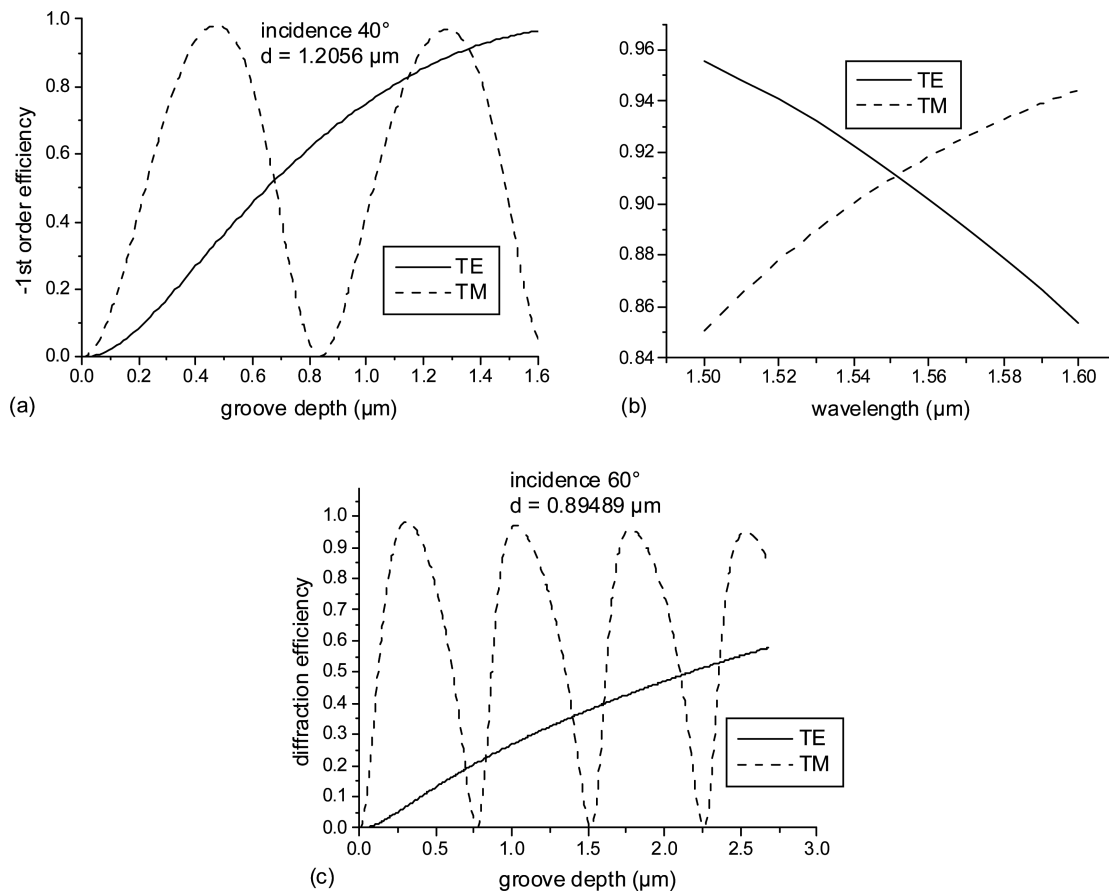


Fig. 1. Efficiency in order -1 of a 1D sinusoidal gold grating. (a) Incidence 40°, period $d = 1.2056 \mu\text{m}$, groove depth dependence at 1.55 μm wavelength. (b) Spectral dependence for $h/d = 1.128$ and parameters from (a). (c) groove depth dependence for an incidence of 60° and period $d = 0.89489 \mu\text{m}$.

(Ox and Oz), although similar performance can be expected with axis inclined at some angle different from 90° . A typical 2D view of the profile is given in Fig. 2 for a set of parameters optimized as explained further.

To work in conditions optimal for wavelength demultiplexing, the 2D-periodic grating needs to work as a 1D grating, i.e., it supports a single dispersive order. The incident working conditions lie close to the xOy plane, as shown in Figs. 3 and 4 for the case of a profile consisting of a set of truncated pyramids. Typically, the design includes some shift off-plane, so that Littrow mount diffraction does not fall into the entry slit (or fiber). This introduces a nonzero angle θ_z between the plane of incidence and the xOy plane (Fig. 3). The period in the x direction is chosen so that the dispersive -1 st order created by this grating goes back close to the incident beam (close to the Littrow mount for the middle of the spectral interval at $1.55\ \mu\text{m}$), but in another plane of diffraction, as presented in Fig. 3, to avoid the incident slit (or fiber).

The period in the perpendicular z direction is chosen so that this second grating cannot create propagating dispersive orders, thus the only two orders that propagate are the zeroth specular order and the -1 st order diffracted by the grating, periodic in the x direction. However, introducing the second grating provides additional degrees of freedom (two more parameters, d_z and h_z), which allow us to enhance the efficiency in TE polarization. In what follows, we define the two fundamental (TE or TM) polarizations as taken with respect to the plane of incidence.

By varying the four possible geometric parameters of the grooves, it is possible to obtain high efficiency in unpolarized light at higher angles of incidence (i.e., higher angular dispersion), when compared to a single-period grating, discussed in Section 2. And indeed, Figs. 5(a) and 5(b) present the spectral dependence of the 2D grating together with the optimal parameters for two different incident angles, 60° and 70° , respectively. In the first case, one observes polarization and spectral variations smaller than 3%, with

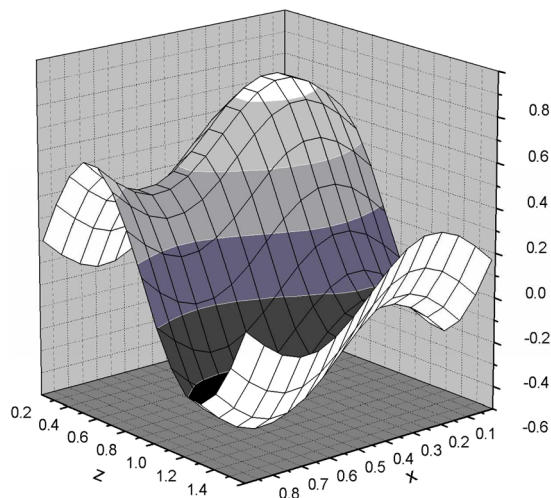


Fig. 2. (Color online) Schematic 2D view of the double-sinusoidal grating with profile given by Eq. (1).

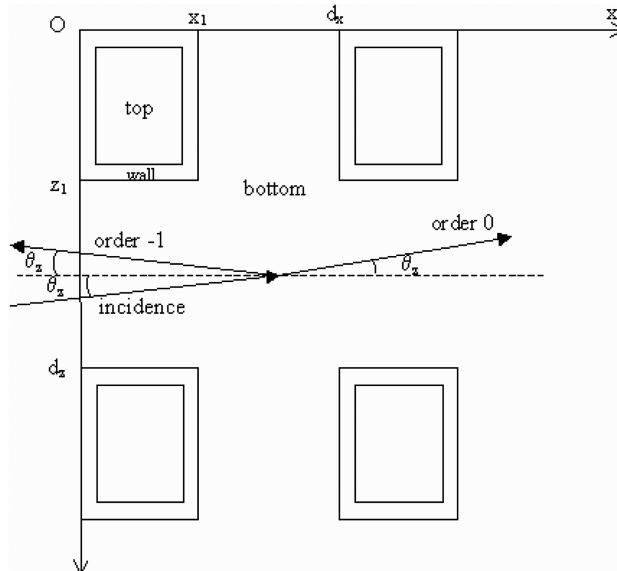


Fig. 3. Top view of a 2D grating made of truncated pyramids (Fig. 4).

mean efficiency higher than 93%. To obtain these results, it is necessary to cover the grating with a 50 nm thin layer of SiO_2 , which increases the efficiency by about 4% when compared to the bare gold surface.

4. Grating Made of Truncated Pyramids

From a technological point of view it could be easier to manufacture gratings having a profile consisting of bumps with almost vertical walls, for example, by chemical or ion-beam etching. Such technology allows for better control of groove parameters when compared with the standard holographic grating recording that results in quasi-sinusoidal profiles.

We tested several different profiles with slope angles varying from 70° to 85° (see Fig. 4), and it is possible to optimize the efficiency behavior by varying the bump dimensions—their height h and the waist at midheight in x and z directions. Two typical examples are given in Fig. 6 for 80° and 70° groove slope angles, respectively. The optimal groove depths are the same, slightly exceeding half of the shorter period. The optimal bump widths vary with the slope

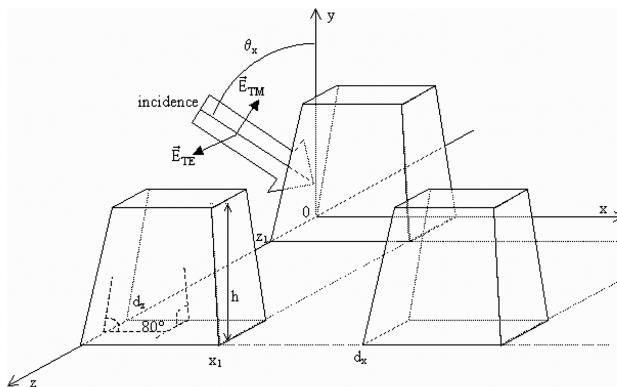
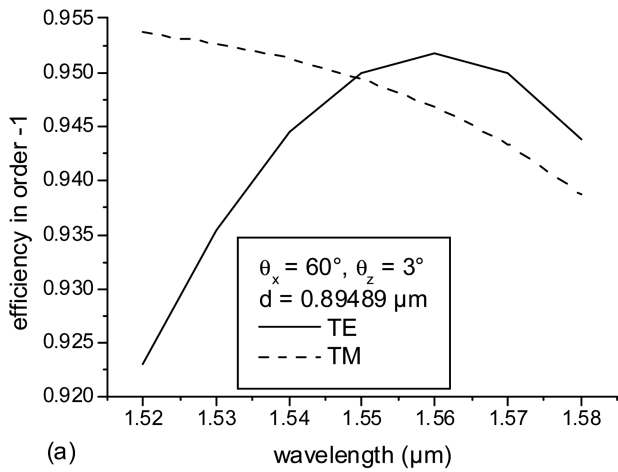
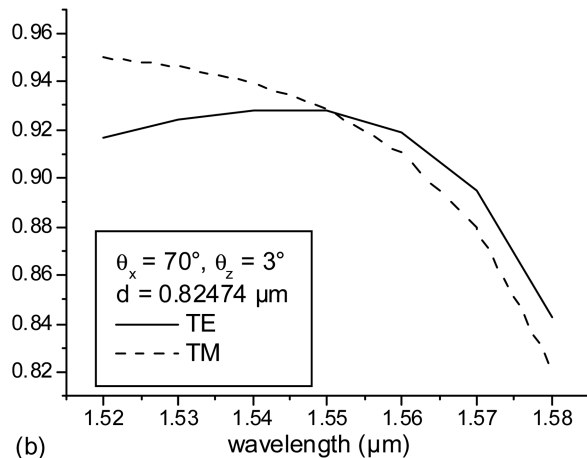


Fig. 4. Side view of a 2D grating made of truncated pyramids.



(a)



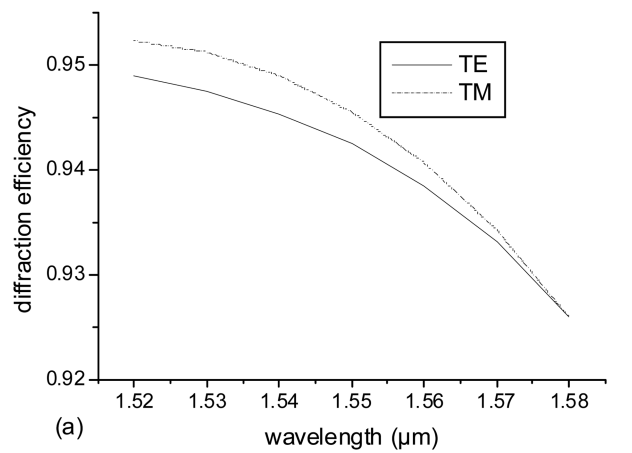
(b)

Fig. 5. Diffraction efficiency of two gratings with profiles given by Eq. (1) and Fig. 2. Gold substrate, covered with a 50 nm thick layer of SiO₂, groove parameters optimized for two different angles of incidence θ_x and 3° off-plane: (a) 60° incidence, $d_x = 0.89489 \mu\text{m}$, $h_x = 0.39 \mu\text{m}$, $d_z = 1.4 \mu\text{m}$, $h_z = 0.88 \mu\text{m}$; (b) 70° incidence, $d_x = 0.82474 \mu\text{m}$, $h_x = 0.3 \mu\text{m}$, $d_z = 1.4 \mu\text{m}$, $h_z = 0.72 \mu\text{m}$.

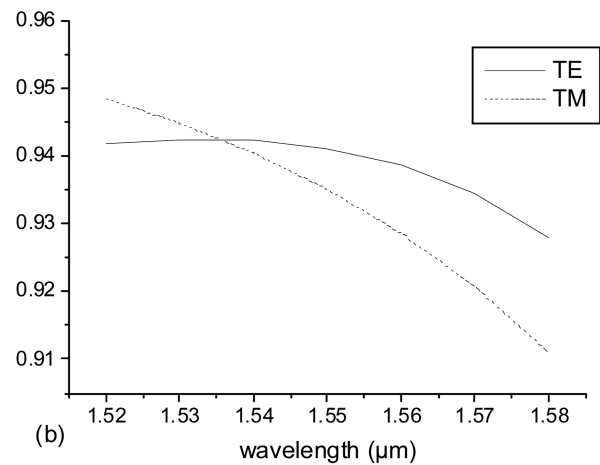
angle, as given in the captions, and must be tuned as a function of the real slope angle obtained during the etching process.

The grating is used close to the Littrow mount, and the wavelength-to-period ratios in both directions allow us to avoid Wood (or other resonance) anomalies, which ensures smooth angular dependences, as shown in Fig. 7 for two different values of the grating period in the x direction, differing by about 1%. As can be observed, such technological error only slightly deteriorates the performance, shifting the maximum from 60° to 61°, which can be expected taking into account that the Littrow position is shifted with the change in the period.

More interesting from a technological point of view are the tolerances with respect to the groove depth and truncated pyramid dimensions because they are more difficult to be maintained than the period. As can be observed in Fig. 8(a), the grating depth tolerances are relatively large, more than 10 nm within 1% change of the efficiency. Such precision can be maintained by using, for example, a stop-etch layer.



(a)



(b)

Fig. 6. Diffraction efficiency of two gratings with profiles given in Figs. 3 and 4. Gold as substrate and bum material, 60° incidence (θ_x) and 3° off-plane: (a) 80° slope of the pyramids, $d_x = 0.89489 \mu\text{m}$, $d_z = 1.4 \mu\text{m}$, bump height $h = 0.49 \mu\text{m}$, bump width at half-height $0.3 \mu\text{m}$ in x , $0.54 \mu\text{m}$ in z ; (b) 70° slope of the pyramids, $d_x = 0.89489 \mu\text{m}$, $d_z = 1.4 \mu\text{m}$, bump height $h = 0.49 \mu\text{m}$, bump width at half-height $0.3 \mu\text{m}$ in x , $0.68 \mu\text{m}$ in z

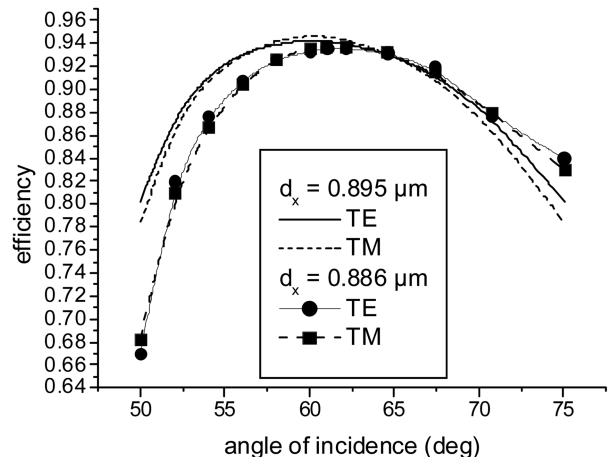


Fig. 7. Angular dependence of -1st order efficiency of the truncated pyramidal grating with parameters presented in Fig. 6(a) for two slightly different periods in the x direction: $d_x = 0.895 \mu\text{m}$ and $d_x = 0.886 \mu\text{m}$, as indicated in the legend. Wavelength $1.55 \mu\text{m}$.

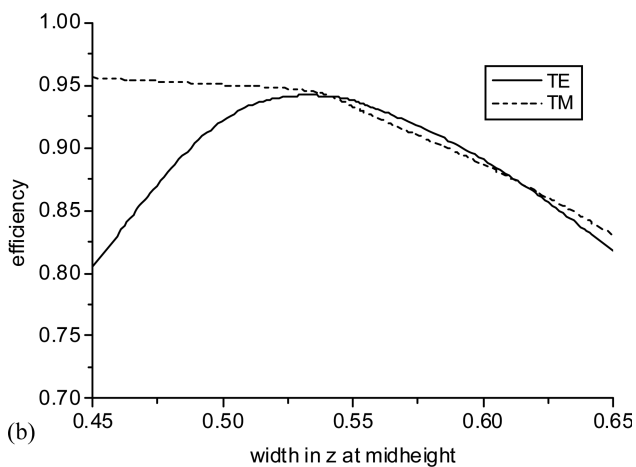
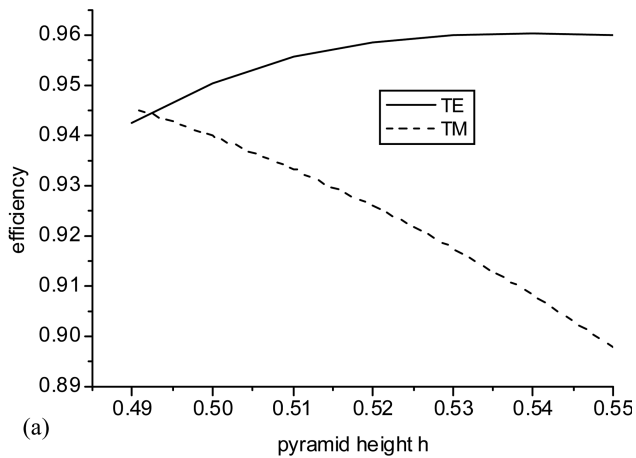


Fig. 8. Tolerance with respect to the structure dimension. The grating parameters are the same as in Fig. 6(a) and the wavelength is equal to $1.55 \mu\text{m}$: (a) groove depth dependence, (b) dependence on the truncated pyramids dimensions in z direction for $h = 0.49 \mu\text{m}$.

The bump width in the z direction must also be kept within 10 nm of the optimal value, as seen in Fig. 8(b), a precision that can be achieved by standard mask etching techniques.

5. Conclusion

Surface-relief gratings having double periodicity in two different directions can be optimized to have high and low-polarization-dependent diffraction efficiency, a property suitable to use for wavelength demultiplexing in unpolarized light. This is possible

with both sinusoidal or truncated pyramidal profiles, having groove parameters achievable by recent manufacturing techniques.

References

1. J.-P. Laude, *Le multiplexage de Longueurs d'Onde* (Masson, 1992).
2. E. Loewen and E. Popov, *Diffraction Gratings and Applications* (Marcel Dekker, 1997).
3. Y. Hao, Y. Wu, J. Yang, X. Jiang, and M. Wang, "Novel dispersive and focusing device configuration based on curved waveguide grating (CWG)," *Opt. Express* **14**, 8630–8637 (2006).
4. P. Muñoz, D. Pastor, and J. Capmany, "The cross waveguide grating: proposal, theory and applications," *Opt. Express* **13**, 2961–2968 (2005).
5. M. Sabeva, E. Popov, and L. Tsonev, "Reflection gratings in the visible region: efficiency in non-polarized light," *Opt. Commun.* **100**, 39–42 (1993).
6. K. Yokomori, "Dielectric surface relief gratings with high diffraction efficiency," *Appl. Opt.* **23**, 2303–2310 (1984).
7. E. Popov, B. Bozhkov, and M. Nevière, "Almost perfect blazing by photonic crystal rod grating," *Appl. Opt.* **40**, 2417–2422 (2001).
8. M. Tekeste and J. Yarrison-Rice, "High efficiency photonic crystal based wavelength demultiplexer," *Opt. Express* **14**, 7931–7942 (2006).
9. T. Matsumoto, Sh. Fujita, and T. Baba, "Wavelength demultiplexer consisting of photonic crystal superprism and superlens," *Opt. Express* **13**, 10768–10776 (2005).
10. B. Momeni, J. Huang, M. Soltani, M. Askari, S. Mohammadi, M. Rakhshandehroo, and A. Adibi, "Compact wavelength demultiplexing using focusing negative index photonic crystal superprism," *Opt. Express* **14**, 2413–2422 (2006).
11. J. Hoose, "Optical diffraction grating structure with reduced polarization sensitivity," U.S. patent 6,487,019 (26 November 2002).
12. J. Hoose, R. Frankel, and E. Popov, "Diffractive structure for high-dispersion WDM applications," U.S. patent 6,496,622 (17 December 2002).
13. E. Popov, J. Hoose, B. Frankel, C. Keast, M. Fritze, T. Y. Fan, D. Yost, and S. Rabe, "Low polarization dependent diffraction grating for wavelength demultiplexing," *Opt. Express* **12**, 269–275 (2004).
14. J. Chandezon, M. T. Dupuis, G. Cornet, and D. Maystre, "Multicoated gratings: a differential formalism applicable in the entire optical region," *J. Opt. Soc. Am.* **72**, 839–846 (1982).
15. E. Popov and L. Mashev, "Convergence of Rayleigh Fourier method and rigorous differential method for relief diffraction gratings," *Opt. Acta* **33**, 593–605 (1986).
16. L. Li and J. Chandezon, "Improvement of the coordinate transformation method for surface-relief gratings with sharp edges," *J. Opt. Soc. Am. A* **13**, 2247–2255 (1996).